Unified first-principle analysis of ultraintense laser-matter interactions: Theory, computations and experiments

Pavel Polynkin
College of Optical Sciences
University of Arizona
Tucson, Arizona

US AFOSR BRI grant #FA9550-12-1-0482

Program goals:

1. Devise first-principle models of the interaction of fs laser pulses with materials (both on surfaces and inside transparent materials);
   implement models in numerical codes

2. Develop non-perturbative ionization models and incorporate them in the codes

3. Conduct experiments to support and verify modeling:
   - Pump-probe imaging of ablation with ultrashort probe (5 fs)
   - Pump-probe imaging of ablation of microdroplets with XUV probe

4. Experimentally study exotic ablation situations:
   - Confined microexplosions inside transparent solids and on interfaces
   - Ablation with ultrashort laser pulses ~5 fs
   - Ablation with fs pulses in the wavelength range 200 nm – 2.6 μm
   - Effects of pulse shaping in ablation

First-principle models of fs laser-matter interactions

<u>Model #1</u> – modeling high-NA fs beam propagating <u>inside</u> a dielectric

Non-paraxial Maxwell propagator coupled with rate equations for ionization and electron heating

Simulate first <100fs → lattice remains cold

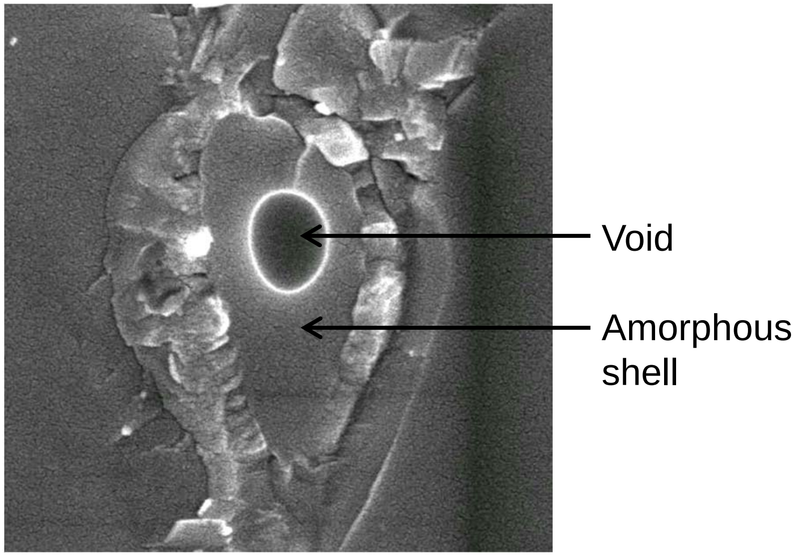

Practical goals:

- Compute distribution of energy absorbed inside dielectric
- Maximize absorbed energy via tailoring beam and pulse shapes
  - → Create larger voids
  - → Create more extreme pressures and temperatures

Computationally challenging – need to resolve significantly sub-wavelength spatial transients (moving skin layers ~ 10 nm – thick at max. ionization)

Preliminary results in full 3D – Brute force approach: Constant grid size < Skin depth

- Full 3D simulation
- 800nm wavelength, 100fs pulse
- Ionization limited at $n_e = 3 \cdot 10^{27}\mathrm{cm}^{-3}$ (~1.5 times critical density, skin depth = 175 nm)
- 32 processors, uniform 20 nm grid, 5 hours computation time

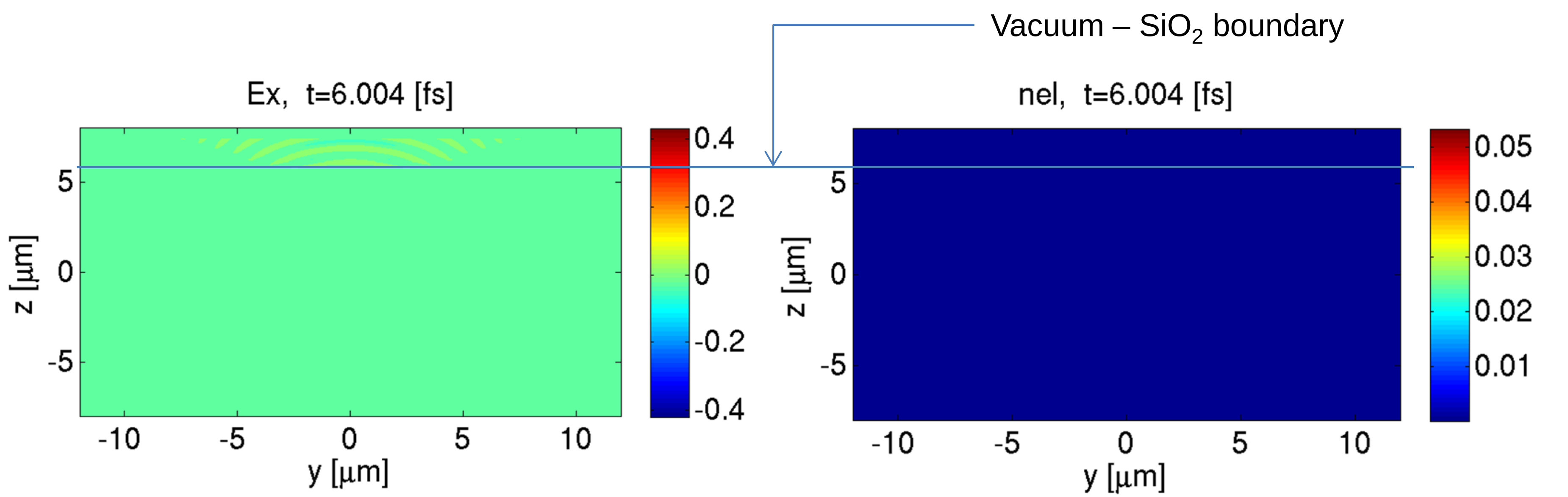

Model #1 – future work

- **Brute force in 3D with full ionization is impractical: ~50 years/computation**
- **Approaches:**
  - **– Variable (but static) grid across computational domain**
  - **– Adaptive grid**
  - **– 2D (x,z,t) - corresponds to cylindrical focusing, axial microexplosion**
  - **– 2D (r,z,t) – corresponds to 3D with azimuthal or radial polarization, realizable through polarization beam shaping with S-plate**

- S-plate is a micro-structured optical polarization converter
- Converts linear into azimuthal or radial polarizations
- Produces large longitudinal field in focus

M. Beresna, M. Gecevicius, P. Kazansky, T. Gertus
"Radially polarized optical vortrex converter created
by femtosecond laser nanostructuring of glass",
APL **98**, 201101 (2011)

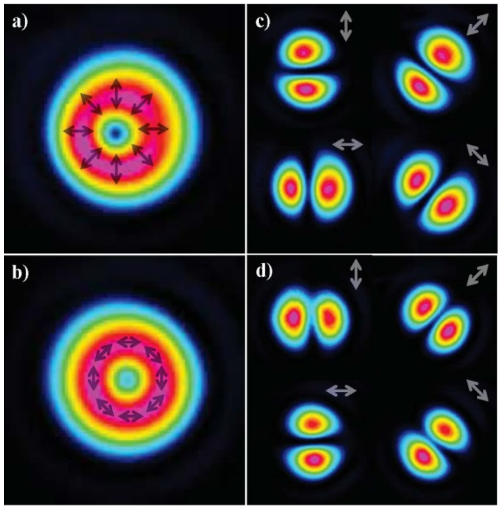

- **Implement different (empirical and rigorous) ionization models in the code**

Empirical ionization model based on rate equations for n_e and T_e & Drude model (Gamaly-Rode):

- Study the regime between ionization and ablation thresholds (ions are not moving)
- Scattering rate depends on electron temperature:
  grows with T_e at low T_e, then $\sim T_e^{-3/2}$ near ablation threshold
- This dependence causes non-trivial dependence of Drude reflectivity on pulse fluence or on time along the pulse

$$\epsilon_{Re} = \epsilon_0 - (\epsilon_0 - 1)\frac{n_e}{n_{at}} - \frac{n_e}{n_{cr}\left[1 + \left({}^{\nu_{eff}(T_e)}/_{\omega}\right)^2\right]}$$

$$\epsilon_{Im} = \frac{n_e}{n_{cr}\left[1 + \left({}^{\nu_{eff}(T_e)}/_{\omega}\right)^2\right]} \cdot \frac{\nu_{eff}(T_e)}{\omega}$$

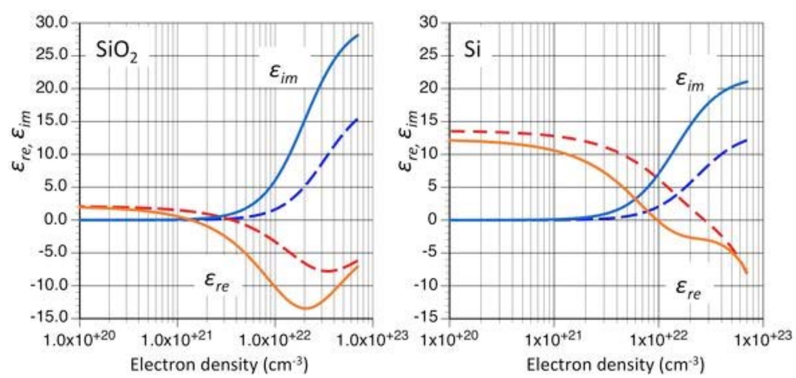

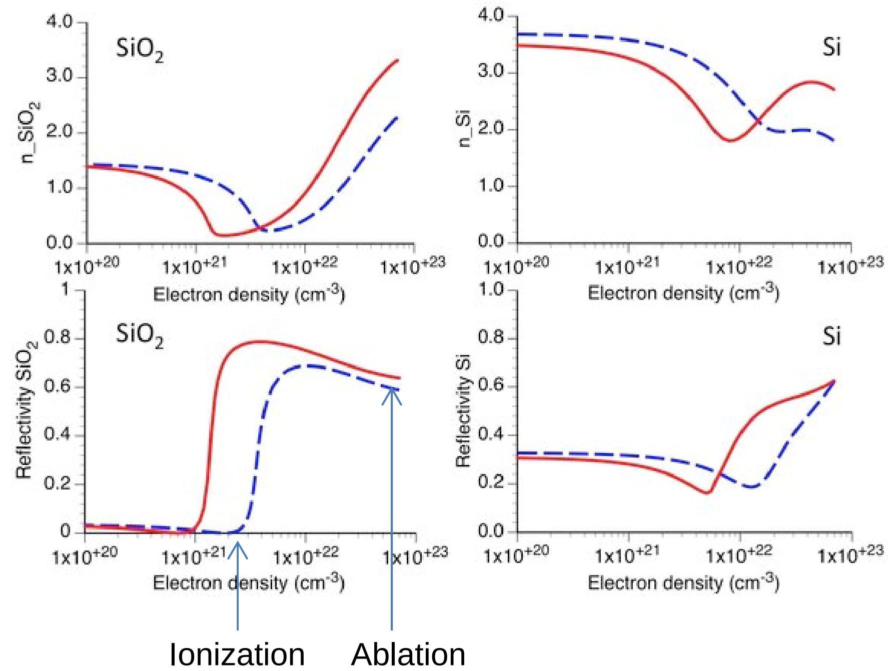

E. Gamaly, A. Rode, “Transient optical properties of dielectric excited by ultra-short laser pulse” (Submited)

Supporting experiments (UA)

Studies of ionization dynamics – regime between ionization and ablation thresholds
Measurements of transient dielectric function (SiO_2)

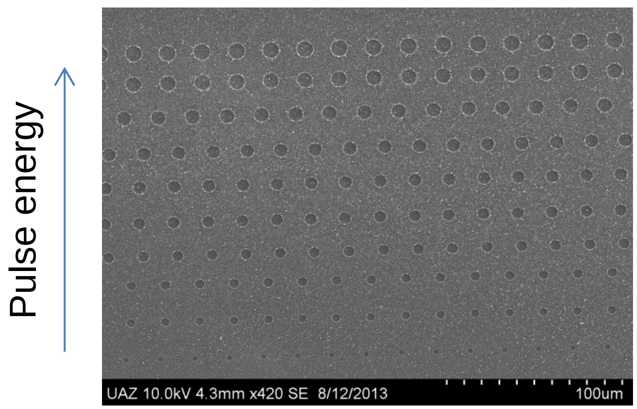

$$F(r) = \int_{-\infty}^{+\infty} e^{-2\left(r/R_{beam}\right)^2} \cdot I(r=0,t) \cdot dt$$

$$F_{th} \approx e^{-2\left(r_{crat}/R_{beam}\right)^2} \cdot \int_{-\infty}^{+\infty} I(r=0,t)dt$$

$$\frac{F(r=0)}{F_{th}} = e^{2\left(r_{crat}/R_{beam}\right)^2}$$

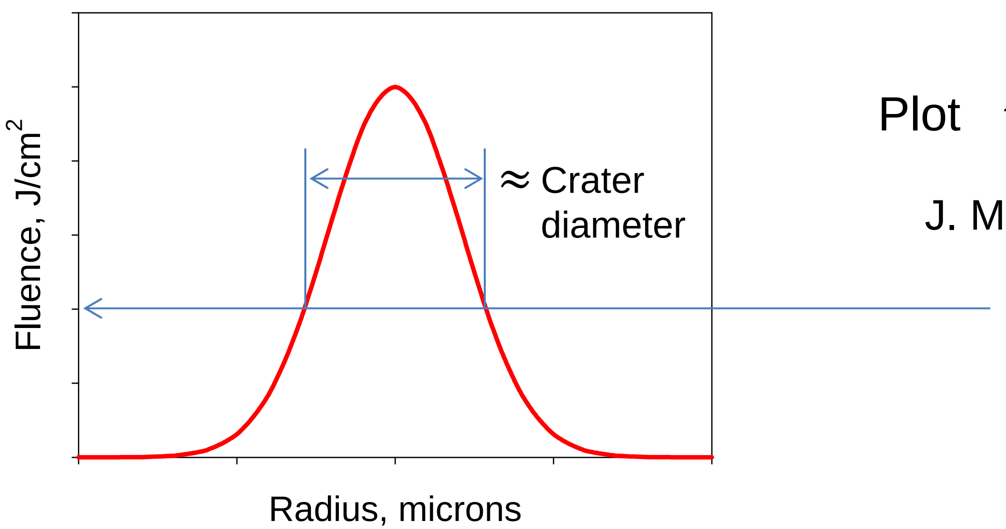

Plot $r_{crat}{}^2$ vs. $\log(F) \implies F_{th},\ R_{beam}$

J. M. Liu, Opt. Lett. **7**, 196 (1982)

Ablation threshold fluence

Supporting experiments (UA)

Studies of ionization dynamics – regime between ionization and ablation thresholds
Measurements of transient dielectric function (SiO_2)

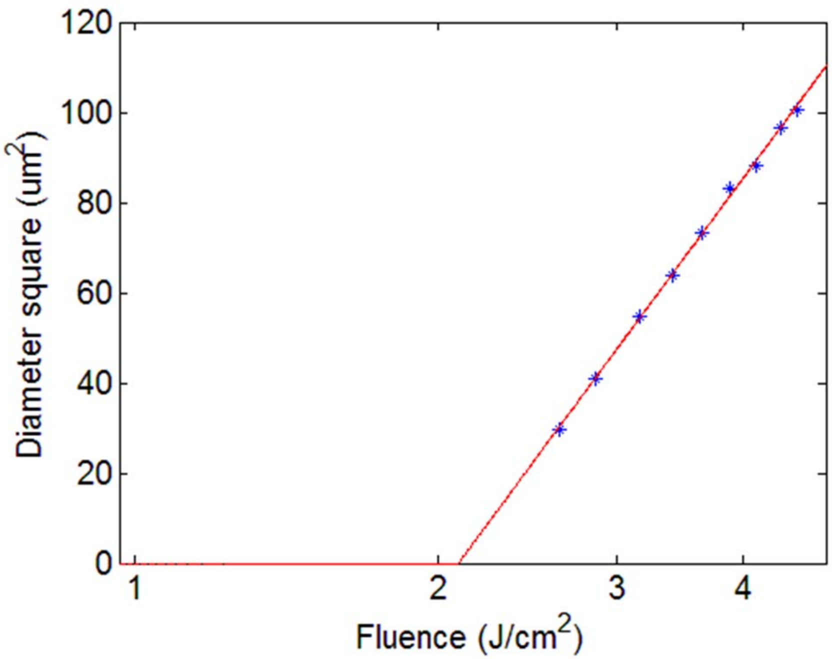

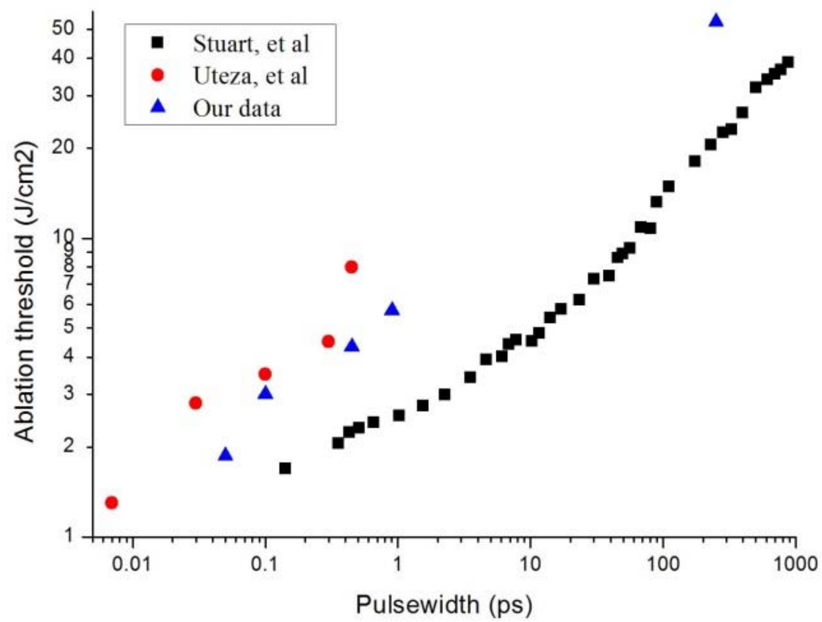

B. Stuart et al. (LLNL), JOSAB **13**, 459 (1996)
O. Uteza et al. (U. Marseille, INRS Quebec), Appl. Phys. A **105**, 131 (2011)

- Ablation threshold fluence 2.1 J/cm^2 for 70 fs pulse
- Beam radius 8.1 μm, consistent with knife-edge measurement

Supporting experiments (UA)

Measurements of ionization threshold – detect anomalies in transmission vs. energy

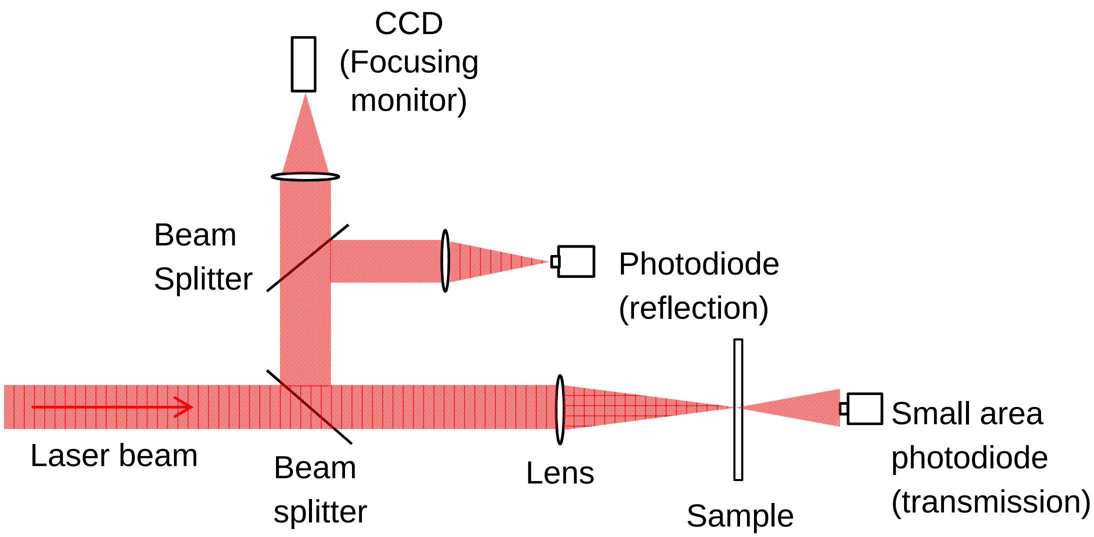

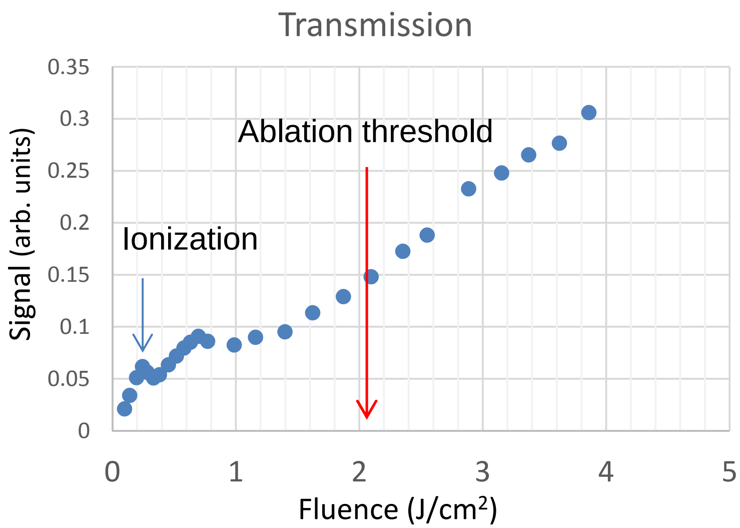

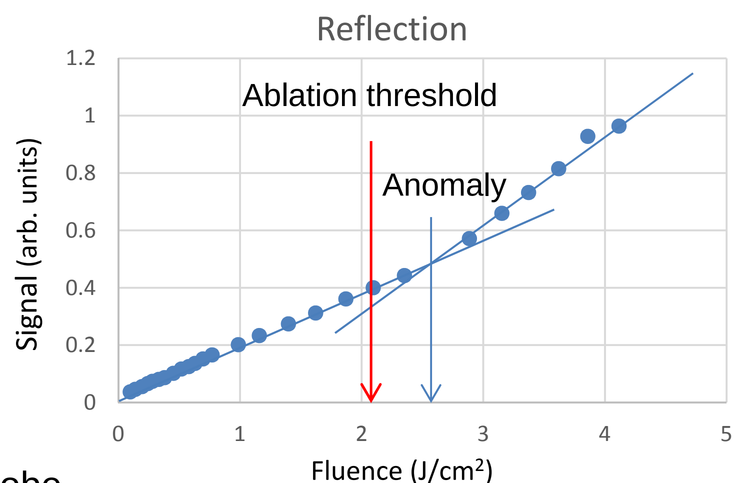

- Measure transmission anomalies in the range 0.2 – 1.0 J/cm^2
- Data is difficult to interpret
- Will conduct pump-probe measurements of reflectivity with 5 fs probe

THE UNIVERSITY OF ARIZONA®

Supporting experiments (UA)

Hollow-fiber pulse compressor installed, being integrated into pump-probe setup.

Will allow transient reflectivity measurements with 5 fs resolution and ablation measurements in the ultrahigh intensity regime

Spectrum

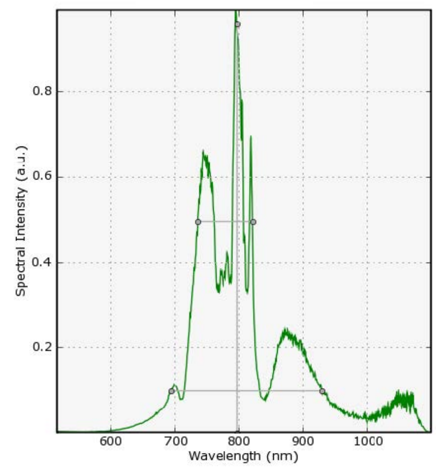

Autocorrelation

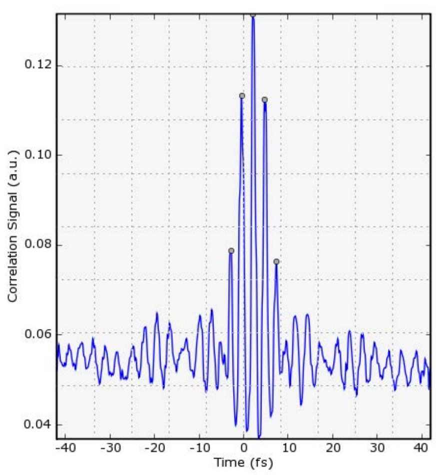

- Neon-filled 100 μm diam. capillary, 1.5 bar.
- Max. compressed output: 0.68 mJ
- Min. pulse duration: 3.7 fringes = 5.1 fs

For ultrahort pulses (<10 fs) and ultrahigh intensities ($>10^{14}$ W/cm^2), sub-cycle effects in ionization become important (M. Ivanov – MBI)

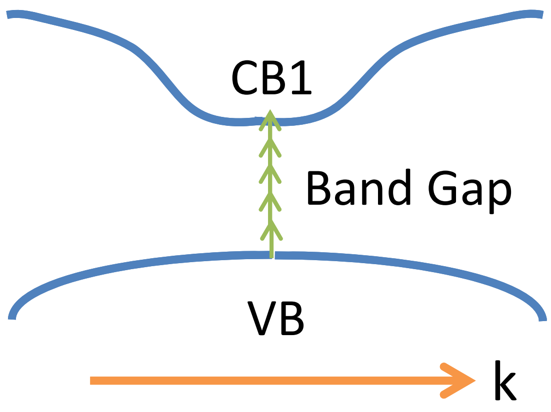

MPI   Avalanche

$$\frac{dn_e}{dt} = \sigma \cdot I^k + \alpha \cdot I(t) \cdot n_e(t)$$

Need non-perturbative treatment

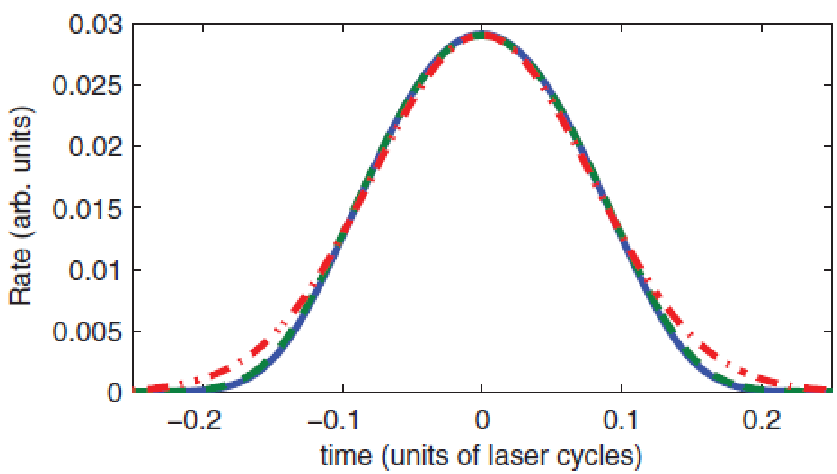

Sub-cycle ionization rate:

- Blue – numerical integration
- Green – approx. analytical formula
- Red – Gaussian fit

Work in progress:

Calibrate analytical formula against absolute cycle-averaged values measured for SiO_2, for incorporation into the Maxwell code

P. Hawkins, M. Ivanov, “Role of subcycle transition dynamics in high-order-harmonic generation in periodic structures”, PRA **87**, 063842 (2013)

Related question: In dielectric crystals, what happens to the band structure in strong IR fields? What is the effective mass of conduction band electrons?

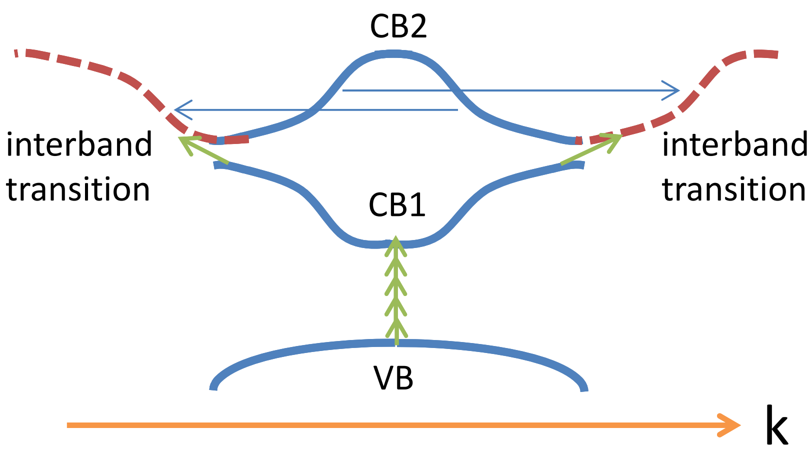

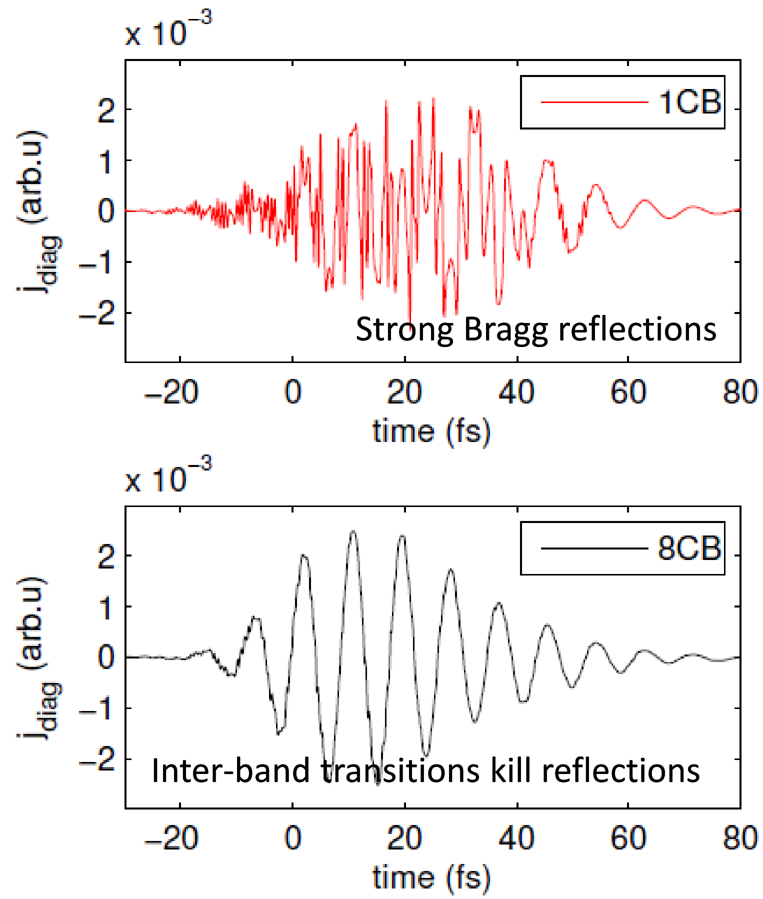

Pilot simulations:
- 1D periodic potential in an IR field
- Solve TDSE with 1valence and different # of conduction bands

Results:
- Strong IR field eliminates band structure, creates a single effective parabolic band
- Conduction band electrons behave like free electrons with effective mass $m=m_0$
- Harmonic generation strongly suppressed

First-principle models of fs laser-matter interactions

<u>Model #2</u> – First-principle model of surface ablation

Quantify relative contributions of Coulomb explosion and electrostatic ablation mechanisms

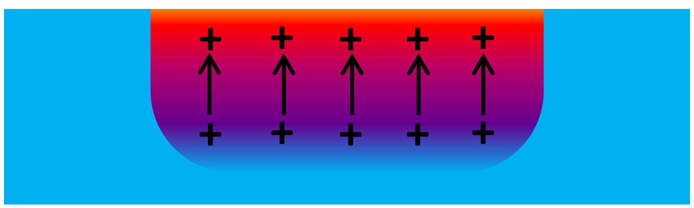

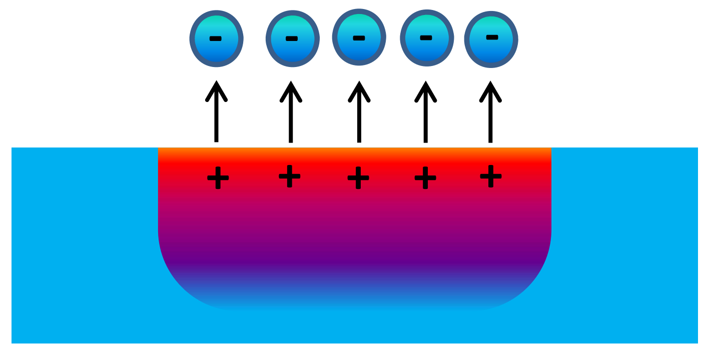

Coulomb explosion: Electrons leave, excessive positive charge pushes ions out of the material.

Some delay between departures of electrons and ions

Electrostatic ablation: Electron sheet pulls ions out of the material.

Electrons and ions leave simultaneously

E. Gamaly, A. Rode, V. Tikhonchuk, B. Luther-Davis, "Electrostatic mechanism of ablation by femtosecond lasers", Appl. Surface Science **197-198**, 699 (2002).

W. Roeterdink, L. Juurlink, O. Vaughan, J. Dura Diez, M. Bonn, A. Kleyn, "Coulomb explosion in femtosecond laser ablation of Si(111)", Appl. Phys. Lett. **82**, 4190 (2003).

Model #2: Kohn & Sham model –

Quantum mechanics for electrons, classical mechanics for ions.

Computationally very challenging
– Can only treat 1D case with ~30 ions on a “conventional” (but still large) computer

- Electrons interact not individually but through the overall electron density *n*(*r*)
- Driving of electrons by external field is described by vector potential *A*(*r*)
- Coulomb interaction is described by total potential *V*(*r*,*t*,*n*), which is the sum of electron and ion potentials
- Motion of individual ions is treated classically

$$i\hbar\frac{\partial}{\partial t}\Psi_j = \frac{1}{2m_e}\left(\frac{\hbar}{i}\vec{\nabla} + e\vec{A}\right)^2\Psi_j + V(\vec{r},t,n)\Psi_j$$

$$V(\vec{r},t,\rho) = e^2\int\frac{n(\vec{r}\,',t)}{|\vec{r}-\vec{r}\,'|}d^3\vec{r}\,' + V_{xc}(n) - e^2\sum_{n=1}^{N_Z}\frac{Z_n}{|\vec{r}-\vec{R}_n|}$$

$$m_n\frac{\partial^2\vec{R}_n}{\partial t^2} = Z_n Z_m e^2\sum_{m\neq n}^{N_Z}\frac{\vec{R}_n-\vec{R}_m}{|\vec{R}_n-\vec{R}_m|^3} + e^2 Z_n\vec{\nabla}_{\vec{R}_n}\int\frac{n(\vec{r},t)}{|\vec{r}-\vec{R}_n|}d^3\vec{r}$$

Compute 1D ground state (prior to arrival of laser pulse)

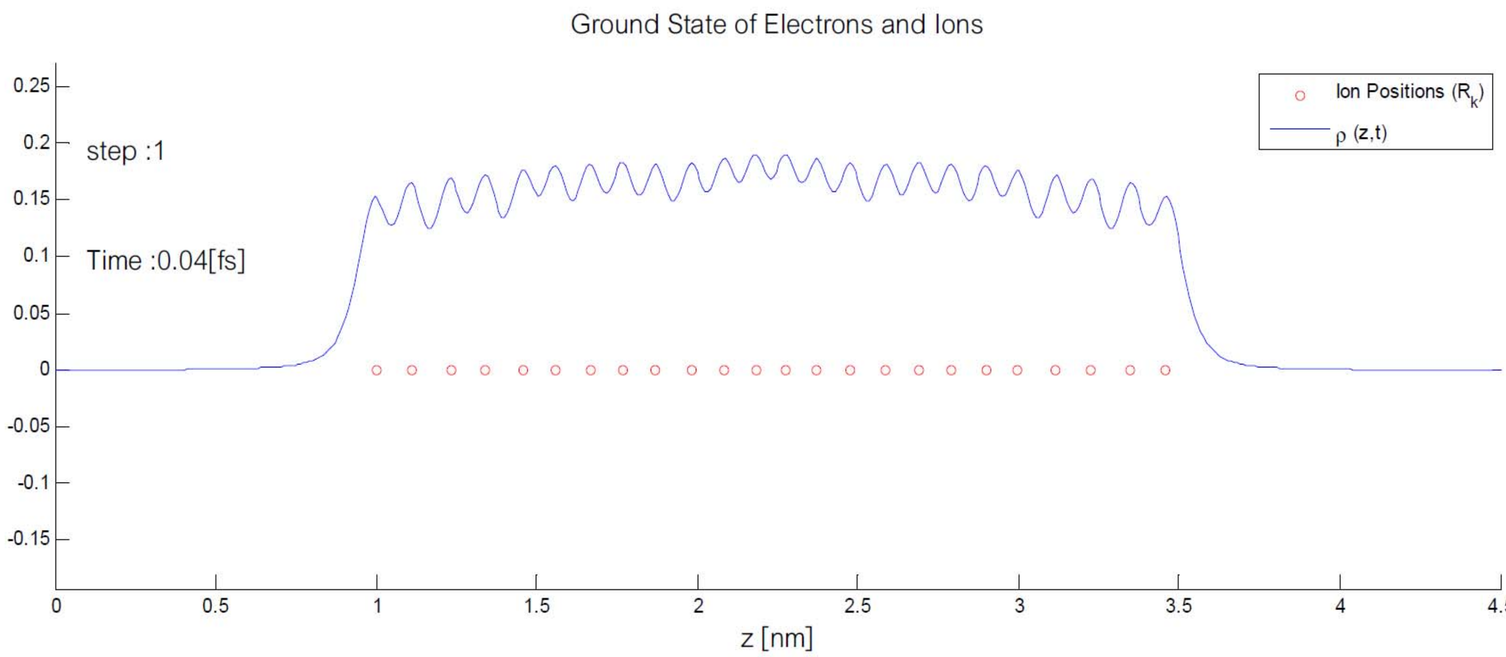

- Computed initial ground state (shown)
- 24 ions (red) are computed, typical distances of ~1.1 Angstroms
- Total electron probability density (blue) computed as sum of 48 electron probability densities

1D string of ions + electrons excited by 20fs laser pulse

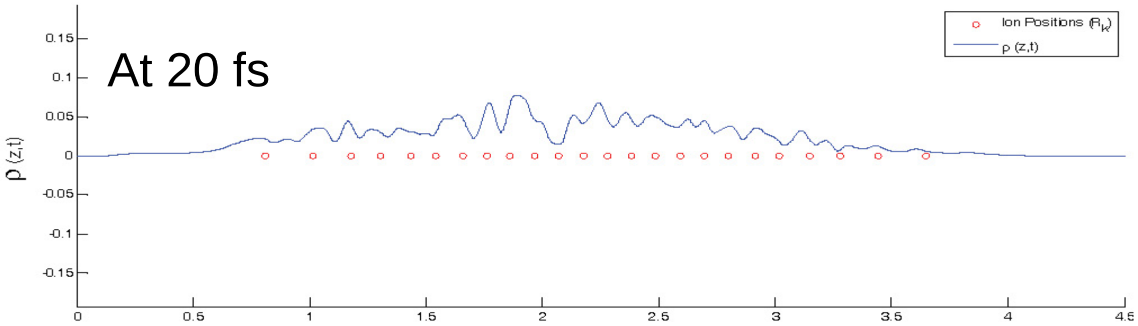

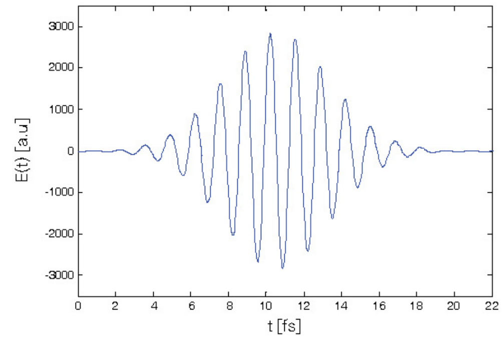

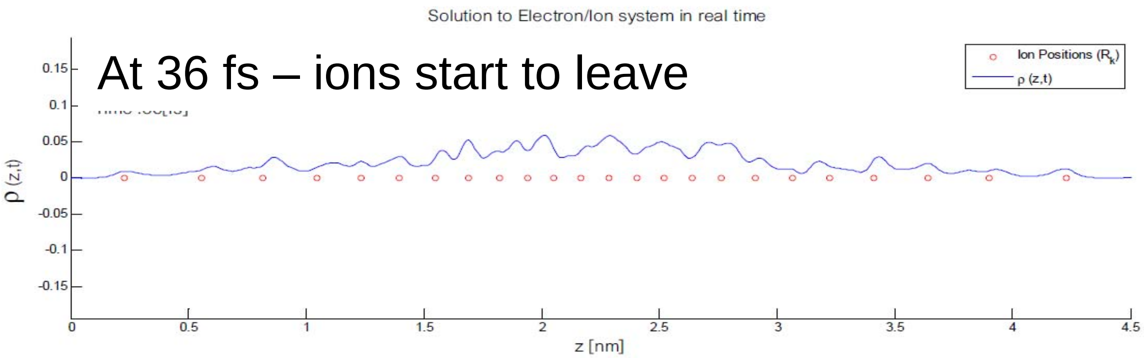

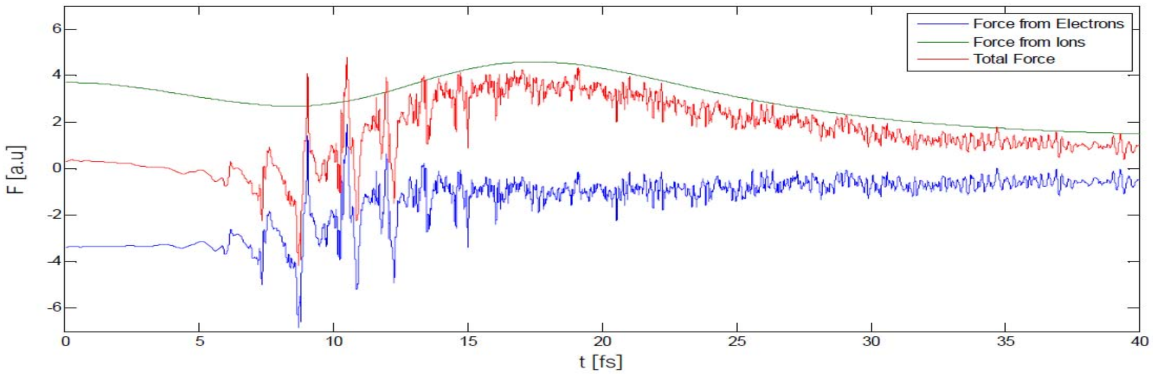

Forces acting on the edge ion – pushing by other ions dominates over pulling by electrons

<u>Coulomb explosion wins in 1D</u>

1D, 2D and 3D cases are qualitatively different

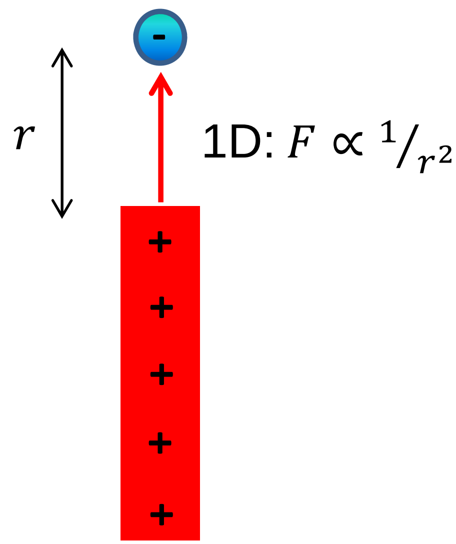

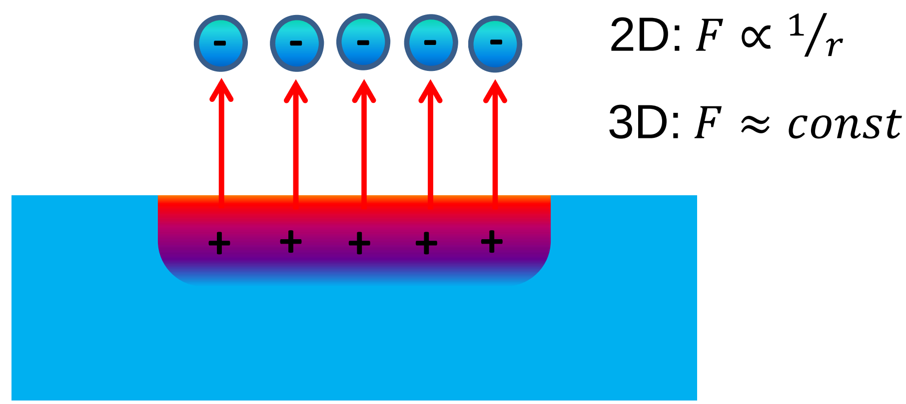

DFT treatment of realistic sample sizes, even in 2D, is impractical:
(800 nm)^2 2D sample contains ~10^7 ions → 5^{18} bytes simulation - huge

On-going work:

- <u>Implement a semi-classical model instead</u>
  - – Electrons and ions are treated as classical particles, with the addition of a velocity-dependent potential preventing electrons falling on ions

(Erik Lotstedt, T. Kato, K. Yamanouchi, "Classical dynamics of laser-driven D3+" (PRL **106**, 203001 (2011))

Supporting experiments
(Hannover – Uwe Morgner, Milutin Kovacev, Heiko Kurz)

So far studied high harmonic generation in water microdroplets driven by pairs of fs pulses separated by several nanoseconds

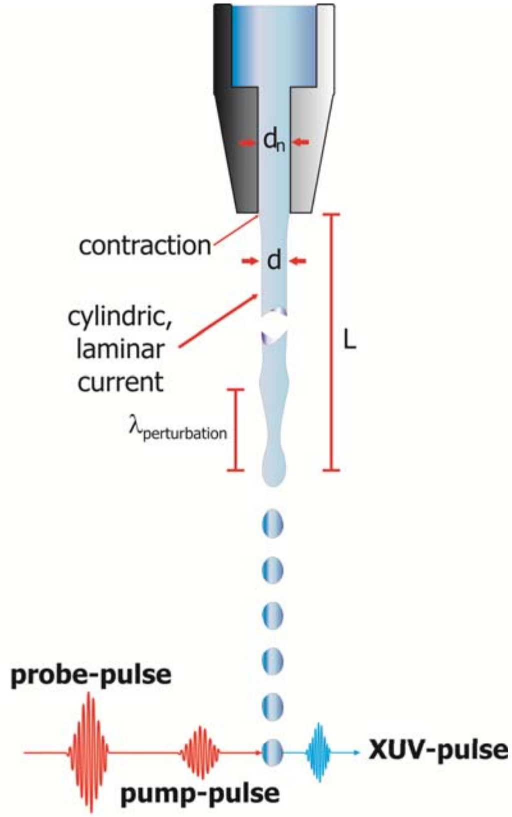

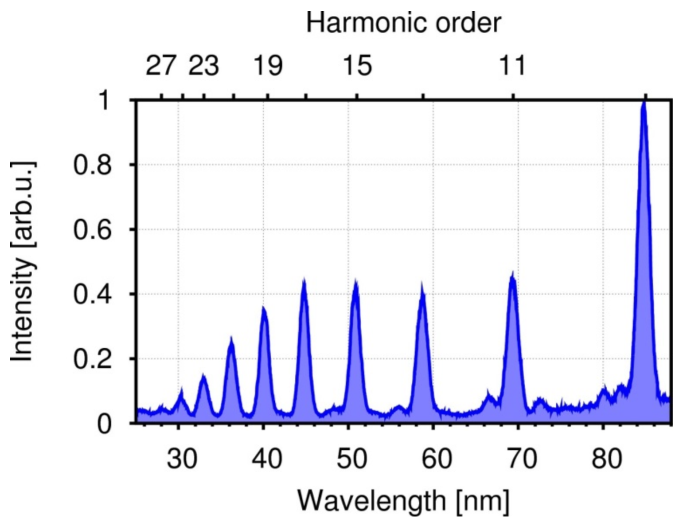

- Pump intensity: 3.7 x 10^{14} W/cm^2 → ~ 40 J/cm^2
- Pump-probe delay: 1 ns
- Harmonics of up to the 27th order generated

H. Kurz, D. Steingrube, D. Ristau, M. Lein, U. Morgner, M. Kovacev,
“High-order-harmonic generation from dense water microdroplets”, PRA **87**, 063811 (2013)

Supporting experiments
(Hannover – Uwe Morgner, Milutin Kovacev, Heiko Kurz)

Imaging of laser ablation of microdroplets in orthogonal pump-probe setup incorporating optical and XUV probe beams

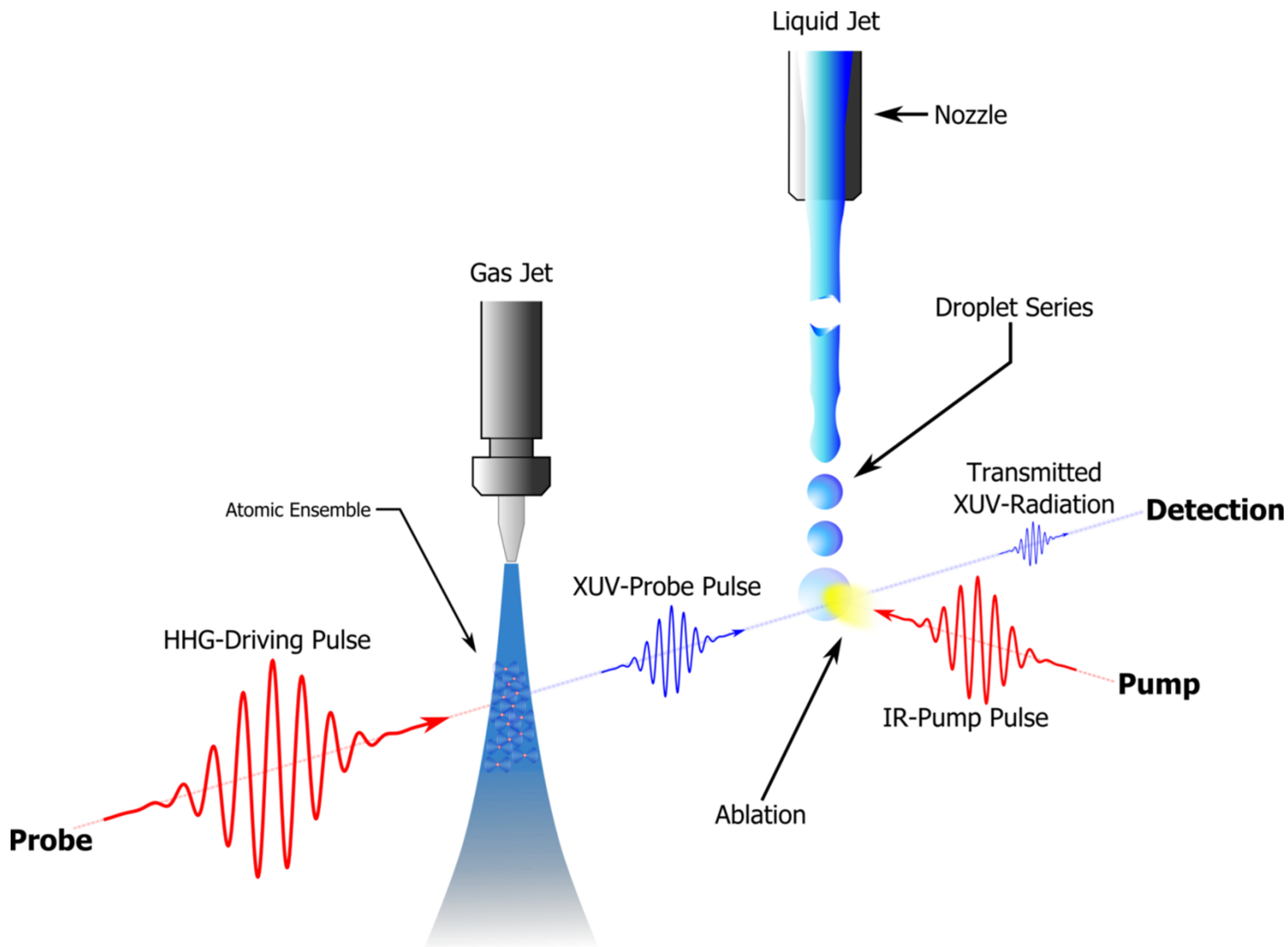

Exotic situations of fs laser-matter interactions

Update on confined microexplosion experiments at ANU:
Creation of new phases of Si through microexplosion on Si-SiO_2 interface
(A. Rode, E. Gamaly, with Chris Pickard from Univ. College London)

Method:

Confined micro-explosion by ultrafast-laser focused in the bulk of transparent material
– conservation of mass

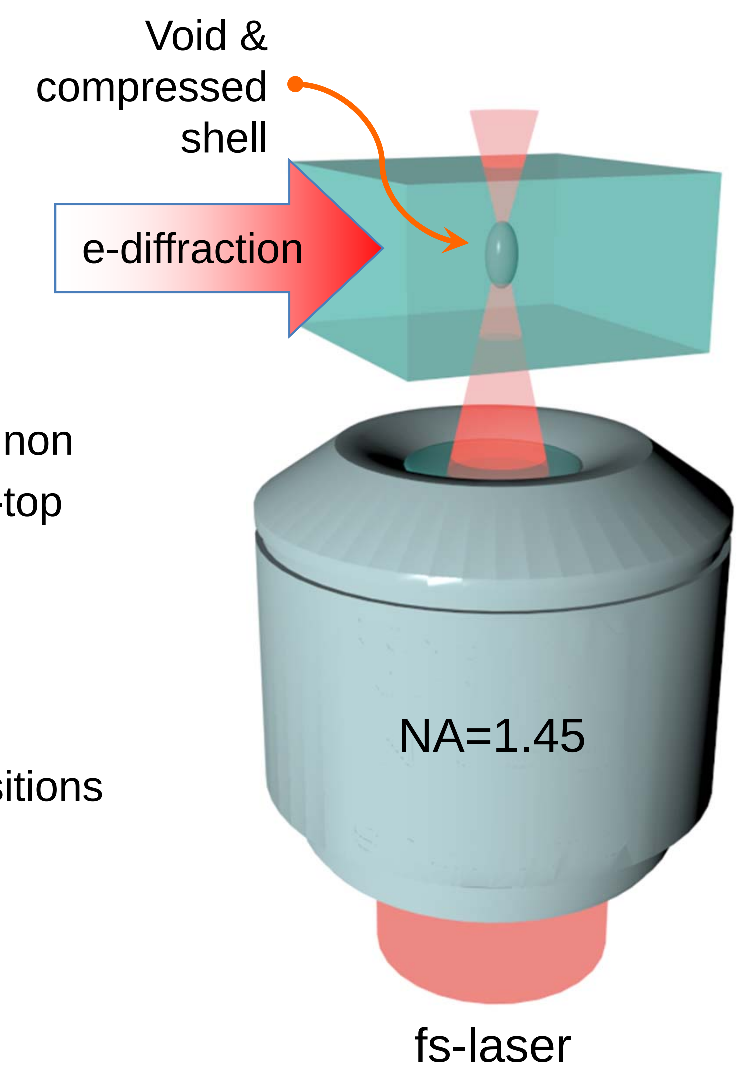

Motivation:

Formation of material states at extreme pressure and non equilibrium temperature conditions in laboratory table-top experiments

Outcome:

- New materials:
  high-pressure ⇔ ultra-hard; insulator-metal transitions
- New material phases (metastable?);
- New chemical/physical
  properties of "shocked" materials

History of microexplosion studies

I – Indication on the creation of high pressure >TPa (10 Mbar) with fs-laser:

E. Glezer, E. Mazur, "Ultrafast-laser driven microexplosion in transparent materials", Appl.Phys. Lett. **71**, 882–884 (1997)

II – Experimental evidence of the >3 TPa pressures in sapphire:

S. Juodkazis, et al., "Laser-induced microexplosion confined in the bulk of a sapphire crystal: Evidence of multimegabar pressures", PRL **96**, 166101 (2006)

III – Discovery of the creation of super-dense material phases inside microexplosion voids:

A. Vailionis, E. Gamaly, V. Mizeikis, W. Yang, A. Rode, S. Juodkazis,
"Evidence of superdense aluminium synthetized by ultrafast microexplosion",
Nature Communications **2**, 445 (2011)

IV – Laser-driven microexplosion on a material interface, densification of opaque materials

L. Rapp, B. Haberl, J. Bradby, E. Gamaly, J. Williams, A. Rode, "Confined microexplosion induced by ultrashort laser pulse at SiO_2/Si interface", Appl. Phys. A **114,** 33 (2014)

Phase transitions of dc-Si to metallic Si

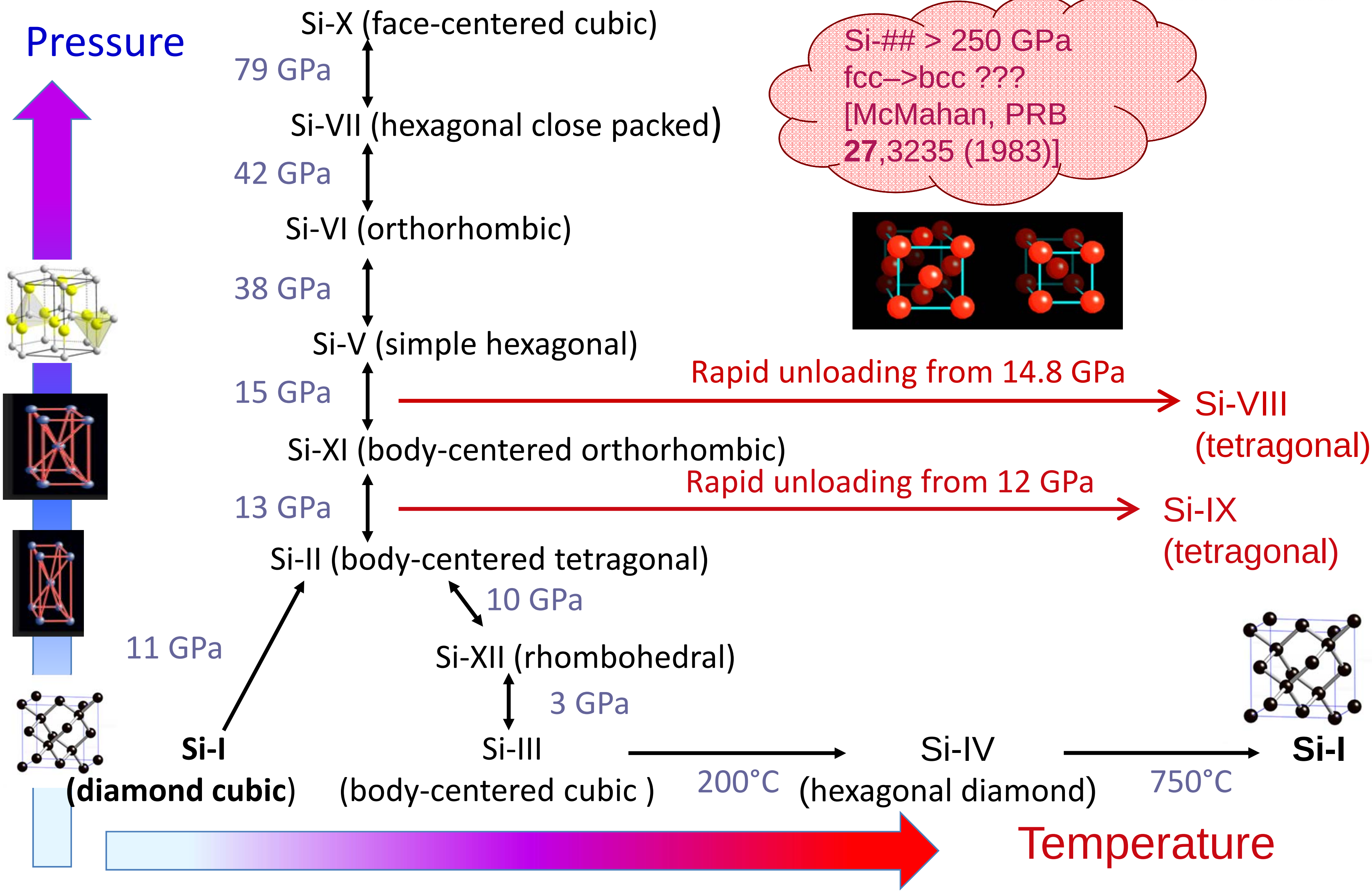

Preparation of samples for TEM and e-diffraction

- Preparation of arrays of micro-explosions ~10 µm under the surface, ~1 µm apart;
- Polishing and cutting to 100-µm thick sample
- Removal of 10-µm thin surface layer with a focused ion beam (FIB)
- Thinning lamella to <100 nm for TEM

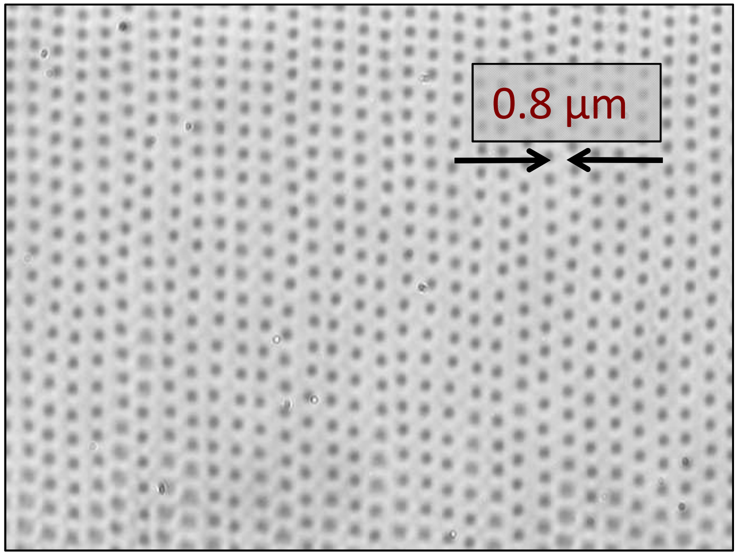

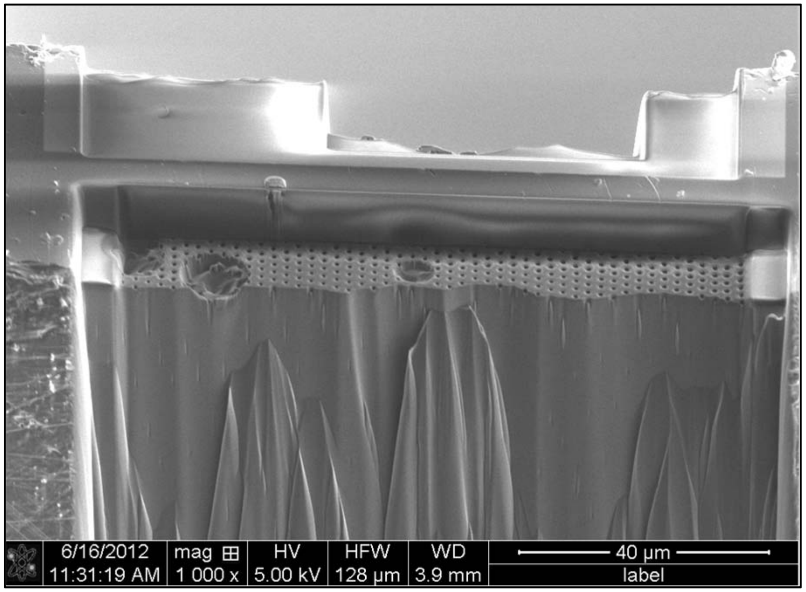

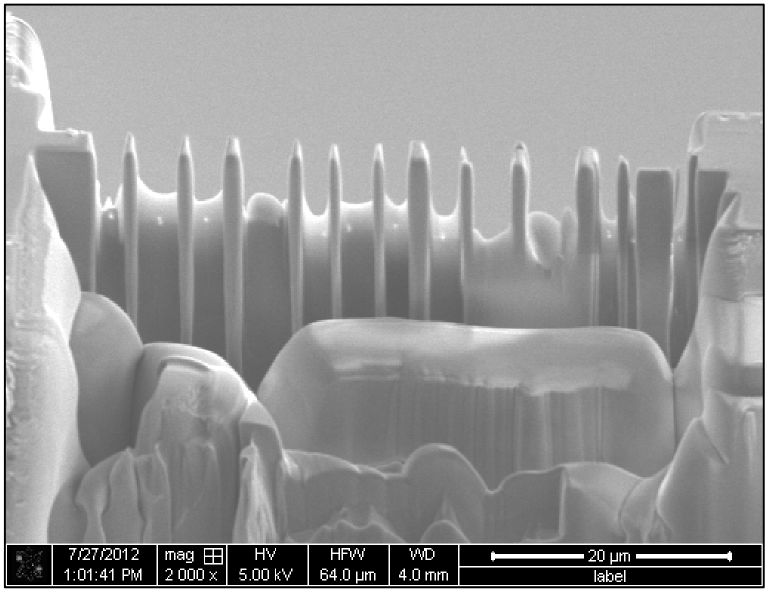

TEM imaging of voids on material interfaces

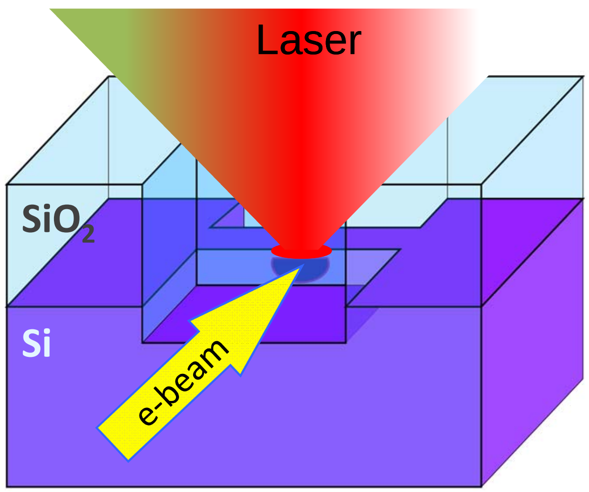

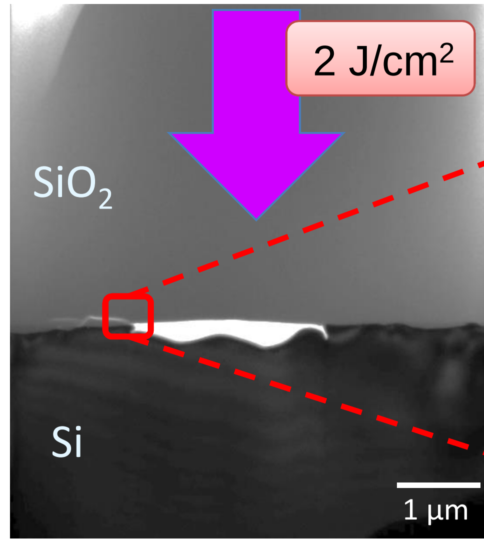

Below threshold
>2 J/cm^2 in SiO_2
(SiO_2 remains intact)

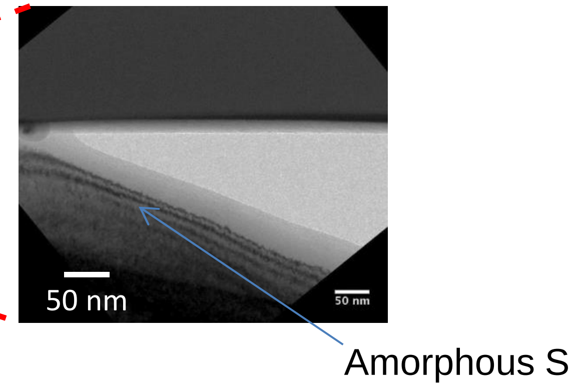

High N.A. with x150

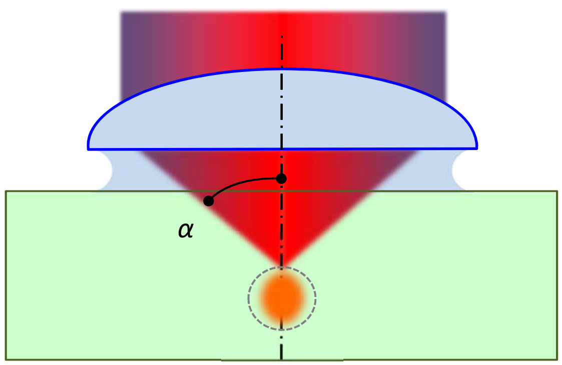

r_f = 0.368 µm

Above threshold in SiO_2
(Absorption in SiO_2)

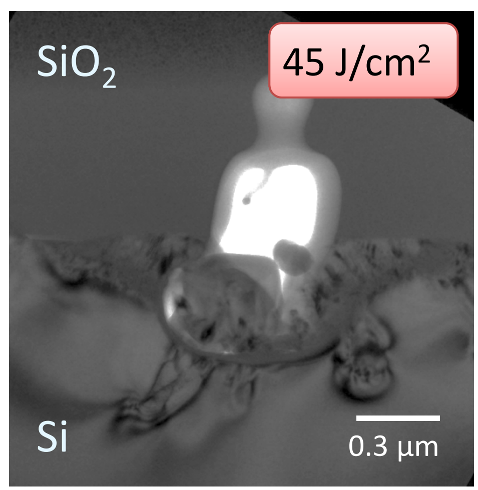

Electron diffraction reveals new material phases

Conventional
diamond-cubic Si

Si
quenched from WDM state

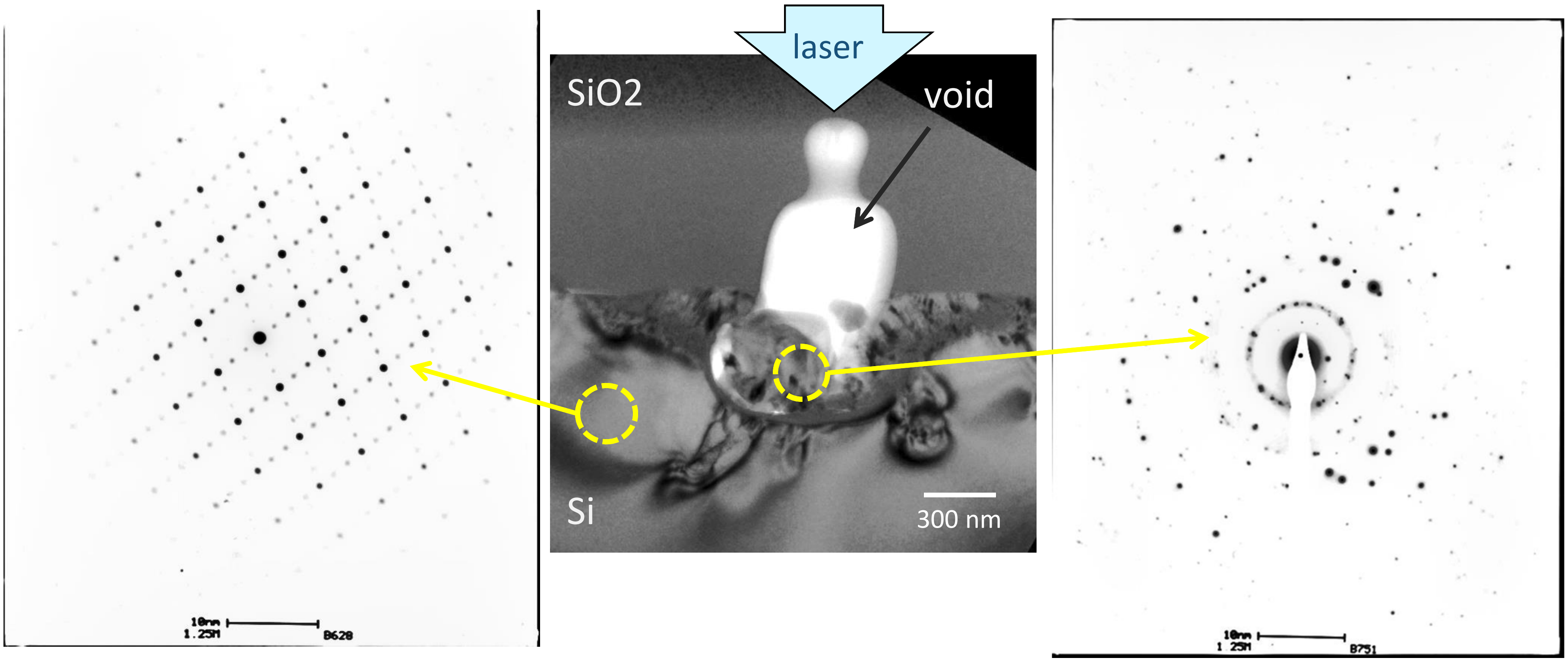

Electron diffraction reveals new material phases

45 J/cm^2

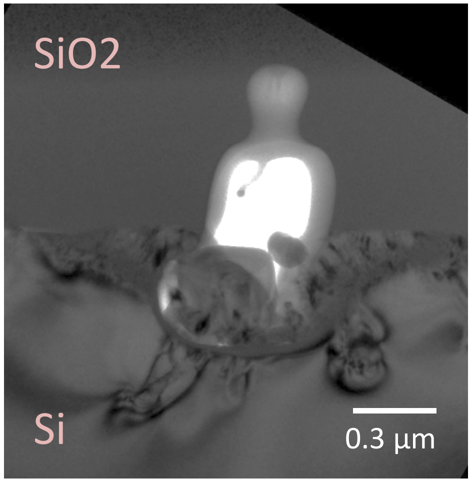

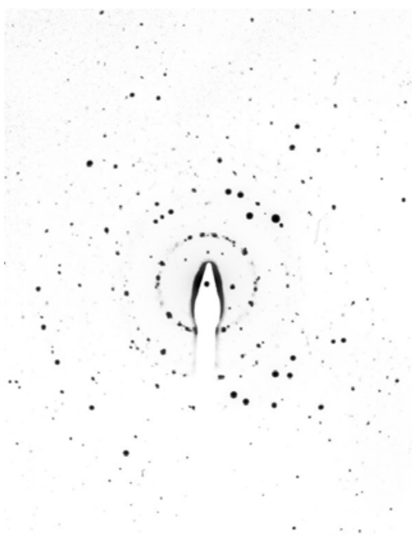

Electron diffraction at 300 kV
data #B751

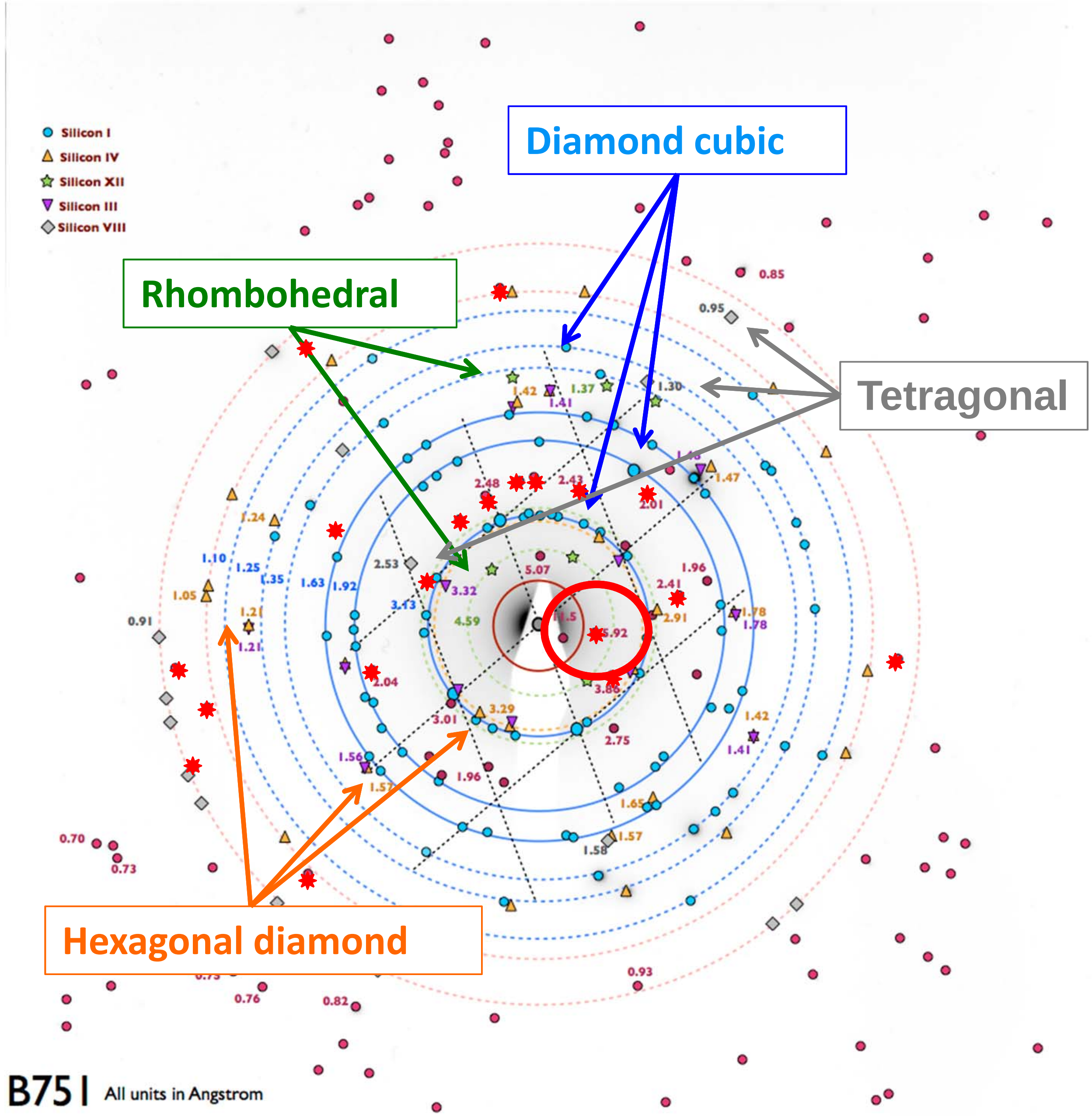

TEM within a particular diffraction order shows spatial locations of new material phases

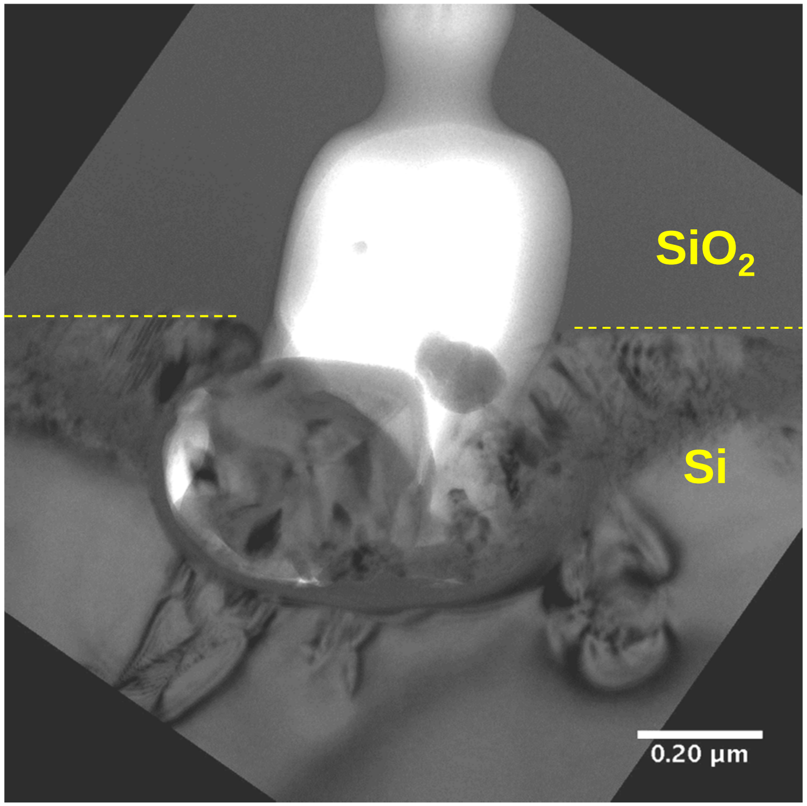

TEM image of void at Si/SiO_2 interface

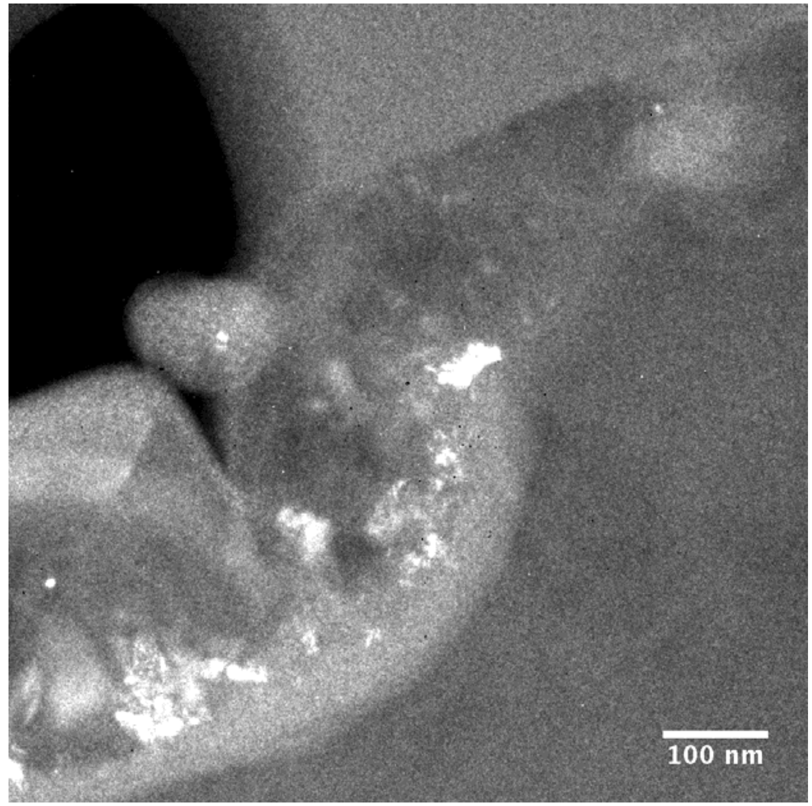

Bright-field image at 5.92 Å bright spot

Results so far:

- First observation of two new tetragonal phases of silicon:
  16-atom Si-BT8 (probably metallic) and 12-atom Si-ST12 (probably narrow-band SC)

- Demonstration of low kinetic barrier in non-equilibrium conditions for formation of new metastable phases – synthesis of phases directly from WDM

- BT8-Si density is 2.73 g/cm^3 at 5 GPa, which is about 17% more dense than dc-Si. Computed density of states indicate the phase is a narrow band gap semiconductor

- ST12-Si density is 2.47 g/cm^3, 6% more dense than dc-Si at ambient pressure. Density of states indicate the phase is an indirect bandgap semiconductor with a bandgap energy between 1.1 eV and 1.67 eV

- These metastable phases are of significant interest, as they may have new electronic and photovoltaic properties

Summary

1. First-principle modeling of fs laser-matter interactions
   - Inside dielectrics: Non-paraxial Maxwell propagator coupled with ionization
   - On surfaces: DFT model of ablation – computationally very challenging, implement a simpler semi-classical model
   - Sub-cycle effects in ionization with ultrashort pulses (<10 fs)
   - Modifications of band structure of crystals in ultraintense laser fields

2. Supporting experiments:
   - Investigations of regimes between ionization and ablation thresholds
   - Measurements of transient reflectivity of ionized dielectrics using 5 fs probe pulse
   - Imaging of ions created through fs ablation of microdroplets with XUV probe

3. Experimental studies of exotic ablation situations:
   - Confined microexplosion inside transparent solids and on interfaces
   - Creation and identification of new super-dense material phases
   - Ablation with ultrashort laser pulses ~5 fs – sub-cycle ionization effects in ablation

THE UNIVERSITY OF ARIZONA

College of Optical Sciences
THE UNIVERSITY OF ARIZONA

ANU
THE AUSTRALIAN NATIONAL UNIVERSITY

MBI

Leibniz Universität Hannover